The Astrophysical Journal, 614:558–567, 2004 October 20

NEAR-INFRARED SPECTROSCOPY OF HIGH-REDSHIFT ACTIVE GALACTIC NUCLEI. II. DISAPPEARING NARROW-LINE REGIONS AND THE ROLE OF ACCRETION

H. Netzer,[1] O. Shemmer,[1] R. Maiolino,[2] E. Oliva,[3] S. Croom,[4] E. Corbett,[4] and L. di Fabrizio[3]

Received 2004 March 28; accepted 2004 June 22

ABSTRACT

We present new near-infrared spectroscopic measurements for 29 luminous high-redshift active galactic nuclei (AGNs) and use the data to discuss the size and other properties of the narrow-line regions (NLRs) in those sources. The high-resolution spectra have been used to carefully model the Fe II blends and to provide reliable [O III] λ5007, Fe II, and Hβ measurements. We find that about two-thirds of all very high luminosity sources show strong [O III] λ5007 lines, while the remaining objects show no or very weak such lines. While weak [O III] λ5007 emitters are also found among lower luminosity AGNs, we argue that the implications for very high luminosity objects are different. In particular, we suggest that the averaging of these two populations in other works gave rise to claims of a Baldwin relationship in [O III] λ5007, which is not confirmed by our data. We also argue that earlier proposed relations of the type $R_{\rm NLR} \propto L_{\rm [O\ III]}^{1/2}$, where $R_{\rm NLR}$ is the radius of the NLR, are theoretically sound, yet they must break down for $R_{\rm NLR}$ exceeding a few kiloparsecs. This suggests that the NLR properties in high-luminosity sources are very different from those observed in nearby AGNs. In particular, we suggest that some sources lost their very large, dynamically unbound NLR, while others are in a phase of violent star-forming events that produce a large quantity of high-density gas in the central kiloparsec. This gas is ionized and excited by the central radiation source, and its spectroscopic properties may be different from those observed in nearby, lower luminosity NLRs. We also discuss the dependence of EW (Hβ) and Fe II/Hβ on luminosity, black hole mass, and accretion rate for a large sample of AGNs. The strongest dependence of the two quantities is on the accretion rate, and the Fe II/Hβ correlation is probably due to the EW (Hβ) dependence on accretion rate. We show the most extreme values measured so far of Fe II/Hβ and address its correlation with EW ([O III] λ5007).

Subject headings: galaxies: active — galaxies: nuclei — galaxies: Seyfert — galaxies: starburst — quasars: emission lines

1. INTRODUCTION

The narrow-line regions (NLRs) of active galactic nuclei (AGNs) have been studied extensively from the ground and from space. This component of the nucleus is spatially resolved from the ground in nearby sources, and *Hubble Space Telescope* (*HST*) observations extend the range to a redshift of about 0.5. Thus, detailed NLR mappings are now available for a large number of sources covering a large range of luminosity and redshift (Falcke et al. 1998; Bennert et al. 2002, hereafter B02; Schmitt et al. 2003).

The spectroscopic characteristics of the NLR gas have been studied extensively over several decades, and high-quality data are now available (e.g., Veilleux & Osterbrock 1987). The main source of excitation of the NLR gas is photoionization by the central continuum (see review and references in Netzer 1990), but shock excitation must be important in some parts of this region, most notably in NLRs that are associated with jetlike radio structures (Schiano 1986; Dopita et al. 2002 and references therein). The gas dynamics have been studied too, with detailed results concerning the profiles of various emission lines and their dependence on the level of ionization, the density, and the dust content of the gas (e.g., Veilleux 1991; Nelson & Whittle 1996; Barth et al. 2001). A major emphasis in recent years has been the extension of such works to higher luminosity sources. Some such studies suggest that the [O III] λ5007 line width is correlated with the stellar velocity distribution in the bulge and thus also with the mass of the central black hole (Nelson 2000; Shields et al. 2003).

Several recent attempts to study NLRs in large samples of AGNs lead to apparently conflicting results. B02 obtained narrowband *HST* images of seven luminous radio-quiet Palomar-Green (PG) quasars with $z < 0.5$. They argued, on the basis of comparison with nearby less luminous sources, that the NLR size (radius) scales with the [O III] λ5007 and the Hβ line luminosities roughly as $R_{\rm NLR} \propto L^{0.5}$. The measured NLR sizes in their most luminous sources approached 10 kpc (throughout this work we assume $H_0 = 70$ km s^{-1} Mpc^{-1}, $\Omega_m = 0.3$, and $\Omega_\Lambda = 0.7$). This dependence has been questioned by Schmitt et al. (2003), who studied a much larger sample (22 Seyfert 1 and 38 Seyfert 2 galaxies), albeit with much lower luminosity, and found $R_{\rm NLR} \propto L^{0.33}$. Croom et al. (2002) analyzed the spectra of $\sim$22,000 AGNs from the Two-Degree Field Quasar Redshift Survey (2QZ) and claimed to see a decrease in the equivalent width (EW) of several narrow lines ([O II] λ3727, [Ne V] λ3426, and [Ne III] λ3870) with source luminosity. They suggested that at least part of this "Baldwin effect" (Baldwin 1977) is due to the increase in NLR size with source luminosity, which leads to galactic scale dimensions in the most luminous objects. Such NLRs are likely to escape the system leading to AGNs with weak or no NLR emission. Testing this idea for the most intense narrow line, [O III] λ5007, was limited

[1] School of Physics and Astronomy and the Wise Observatory, Raymond and Beverly Sackler Faculty of Exact Sciences, Tel Aviv University, Tel Aviv 69978, Israel; netzer@wise.tau.ac.il, ohad@wise.tau.ac.il.

[2] INAF–Osservatorio Astrofisico di Arcetri, Largo Enrico Fermi 5, I-50125 Florence, Italy; maiolino@arcetri.astro.it.

[3] Istituto Nazionale di Astrofisica, Centro Galileo Galilei, and Telescopio Nazionale Galileo, P.O. Box 565, E-38700 Santa Cruz de la Palma, Spain; oliva@tng.iac.es.

[4] Anglo-Australian Observatory, P.O. Box 296, Epping, NSW 1710, Australia; scroom@aaoepp.aao.gov.au.

by the low redshift and hence relatively low luminosity in the Croom et al. (2002) ground-based sample.

This paper addresses the issues of "the disappearing NLRs" and the Fe II/Hβ ratio in high-luminosity AGNs. The work complements the Shemmer et al. (2004, hereafter Paper I) study and is based on the same data set. The paper is arranged as follows: § 2 presents the new observations; § 3 shows various correlations involving the [O III] λ5007, Hβ, and Fe II lines; and § 4 discusses the implications regarding the size and the physics of the NLR as well as the Fe II/Hβ ratio in the most luminous AGNs.

2. OBSERVATIONS

We obtained new near-infrared (IR) spectroscopic observations for a sample of 29 high-redshift, high-luminosity AGNs at the Anglo-Australian Telescope (AAT) in Australia and at Telescopio Nazionale Galileo (TNG) in Spain. The observations and data reduction are described in Paper I, where all IR spectra are also shown (see their Figs. 1–3).

In this work we focus on the [O III] λ5007 emission line, which when observed is the strongest narrow line in the spectrum (all numbers given in this paper refer to the 5007 Å component *only*). We also show and discuss various correlations involving the broad Fe II lines. The measurement of the [O III] λ5007 line is complicated because of the presence of strong, broad Fe II blends in this part of the spectrum. The accurate modeling of these blends is crucial to our study of the Fe II spectrum as well as the measurement of the [O III] λ5007 line. Below we give a detailed description of this process and illustrate the results for the case of [HB 89] 1346−036.

The near-IR spectrum of the quasar [HB 89] 1346−036 ($z = 2.370$) was observed by McIntosh et al. (1999). The same observation was later used by Yuan & Wills (2003), who remeasured the McIntosh et al. (1999) spectrum and used it in their study of the Eddington ratio in $z \sim 2$ quasars. Both McIntosh et al. (1999) and Yuan & Wills (2003) found an [O III] λ5007 line in this source, which was later used in several of their correlations. Our superior, high-S/N, better resolution IR spectroscopy of the source shows broad lines due to Hβ and Fe II and a weak emission feature very close to the putative [O III] λ5007 position (Fig. 1, *top curve*). We have used the empirical Fe II emission template of Boroson & Green (1992, hereafter BG92), scaled to the intensity of the strongest iron features in order to remove those Fe II lines. The broadened template is shown in the diagram, and the Fe II subtracted spectrum is given below the original spectrum. As seen in the diagram, the process completely removed all trace of [O III] λ5007 emission. We applied a similar procedure to the spectra of all other sources, and the results listed below are all corrected for the Fe II blends. We suspect that other sources in the McIntosh et al. (1999) and the Yuan & Wills (2003) samples suffer from a similar problem and hence decided not to include these objects in our analysis. We note that Sulentic et al. (2004) also question some of the McIntosh et al. (1999) measurements.

Table 1 gives a summary of the data used in this paper. It includes the object name (col. [1]), systemic redshift (col. [2]), continuum luminosity defined as λL_λ at rest wavelength 5100 Å (col. [3]), and the basic [O III] λ5007 line measurements (rest-frame EW in cols. [4] and [5], luminosity in cols. [6] and [7], and FWHM in cols. [8] and [9]). Table 1 also gives the best-fit Hβ luminosity in column (10) and the Fe II/Hβ flux ratio[5] in column (11). Regarding the uncertainties on those numbers, some of those are discussed in Paper I, and the others, related to the [O III] λ5007 line, were obtained using the procedure explained in Paper I as applied to this line.

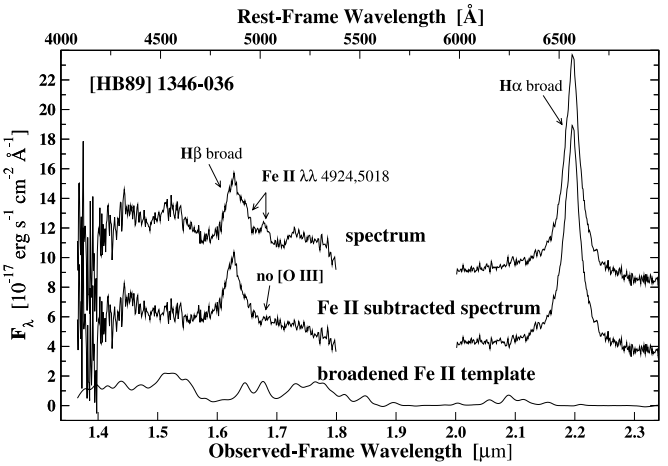

FIG. 1.—Example of the [O III] λ5007 line measurement process for the $z = 2.370$ quasar [HB 89] 1346−036 we observed at TNG in 2002. The diagram shows the reduced calibrated spectrum with emission lines resembling the [O III] λ5007 doublet (*top curve*) and the Fe II-subtracted spectrum (*middle curve*), where no sign of [O III] λ5007 is seen. The Fe II template is also shown (*bottom curve*).

The main result, which is apparent in Table 1, is that the population of high-redshift, high-luminosity quasars is divided into two distinct groups. One group (22 sources) contains objects with strong [O III] λ5007 lines (EW $\sim$ 10−80 Å) and with I ([O III] λ5007)/I (broad Hβ) similar to the ratio observed in many low-luminosity type 1 AGNs. The second group (seven sources) shows *no* [O III] λ5007 *line* within the observational uncertainty. To obtain the upper limits on EW ([O III] λ5007) in those sources, we assumed a "typical" [O III] λ5007 line with FWHM of 1000 km s^{-1} (about the median in our sample; see below) and looked for the weakest such feature that would have been detected in our spectra after the removal of the Fe II blends. For the best S/N spectra (three sources), this translates to an EW that is approximately 0.05EW (Hβ). For the other four cases the upper limits correspond to 0.1−0.2EW (Hβ). The luminosities corresponding to these upper limits are listed in Table 1.

The division into two distinct groups of very high luminosity AGNs is further confirmed by the Dietrich et al. (2002a) observations. These authors found that two of the six luminous $z \simeq 3.5$ quasars in their sample have prominent [O III] λ5007 lines, while the remaining four had no trace of this line. Combining with our new data we find that out of 35 high-luminosity quasars, 24 show strong [O III] λ5007 and 11 others are consistent with no such line in their spectrum.

We have checked this finding in various ways. In particular, we have examined the distribution of I ([O III] λ5007)/I (Hβ), which is shown in Figure 2. The histogram is made up of a broad distribution centered at about 0.3 and a group of sources with I ([O III] λ5007)/I (Hβ) < 0.1. Unfortunately, the uncertainty on the upper limit of I ([O III] λ5007) in two of the sources is very large, and those objects bridge the gap between the strong and the very weak [O III] λ5007 emitters. We must therefore consider two hypotheses: one is a real dichotomy in the [O III] λ5007 line intensity, and the other is a continuous distribution in EW ([O III] λ5007), which has a long tail at very small EWs.

[5] This ratio matches the BG92 definition of R Fe II, i.e., the ratio between the EW of the Fe II blends in the λ4434–λ4684 band and EW (Hβ).

TABLE 1
CONTINUUM AND EMISSION-LINE MEASUREMENTS

QUASAR NAME (1)	z[a] (2)	$\log \lambda L_\lambda(5100)$ (ergs s^{-1}) (3)	EW ([O III]) Best Fit (Å) (4)	EW ([O III]) Direct (Å) (5)	$\log L_{[O\ III]}$ Best Fit (ergs s^{-1}) (6)	$\log L_{[O\ III]}$ Direct (ergs s^{-1}) (7)	FWHM ([O III]) Best Fit (km s^{-1}) (8)	FWHM ([O III]) Direct (km s^{-1}) (9)	$\log L_{H\beta}$, BEST FIT (ergs s^{-1}) (10)	Fe II/Hβ (11)
2QZ J001221.1−283630	2.339	46.26	<10	...	<43.59	...	...	...	44.29	1.27
2QZ J002830.4−281706	2.401	46.58	32	31	44.40	44.38	1511	1823	44.63	0.37
UM 667	3.132	46.28	16	16	43.78	43.79	759	1468	44.44	2.08
LBQS 0109+0213	2.349	46.80	25	31	44.50	44.59	1398	1341	44.93	0.14
[HB 89] 0123+257	2.369	46.57	27	27	44.31	44.32	587	532	44.75	0.26
2QZ J023805.8−274337	2.471	46.57	<7	...	<43.70	...	...	...	44.70	1.57
SDSS J024933.42−083454.4	2.491	46.38	27	27	44.11	44.10	815	394	44.54	<0.1
[HB 89] 0329−385	2.435	46.71	20	24	44.30	44.37	491	450	44.82	0.30
[HB 89] 0504+030	2.473	46.32	73	74	44.49	44.51	1065	836	44.38	0.49
SDSS J100428.43+001825.6	3.046	46.44	54	60	44.46	44.51	527	996	44.76	0.59
TON 618	2.226	47.31	<3	...	<44.11	...	...	...	45.42	0.65
[HB 89] 1246−057	2.240	47.16	<5	...	<44.14	...	...	...	45.14	1.20
[HB 89] 1318−113	2.306	46.89	14	13	44.31	44.28	1903	2303	44.84	<0.1
[HB 89] 1346−036	2.370	46.88	<3	...	<43.72	...	...	...	45.02	0.87
SDSS J135445.66+002050.2	2.531	46.49	<3	...	<43.22	...	...	...	44.52	0.63
UM 629	2.460	46.56	35	23	44.40	44.23	1413	929	44.77	1.29
UM 632	2.517	46.54	15	16	44.03	44.05	196	492	44.85	0.35
UM 642	2.361	46.29	11	14	43.63	43.74	1696	1859	44.53	0.41
UM 645	2.257	46.31	23	30	43.98	44.09	525	633	44.67	0.10
SBS 1425+606	3.202	47.38	23	19	45.03	44.96	1382	659	45.37	0.34
SDSS J170102.18+612301.0	2.301	46.34	<7	...	<43.50	...	...	...	44.50	1.06
SDSS J173352.22+540030.5	3.428	47.00	11	8	44.34	44.22	1335	833	44.99	0.39
[HB 89] 2126−158	3.282	47.25	13	9	44.64	44.51	1327	1040	45.47	0.49
[HB 89] 2132+014	3.199	45.77	59	52	43.83	43.77	1315	1328	44.27	0.54
2QZ J221814.4−300306	2.389	46.54	12	13	43.94	43.96	1791	2343	44.54	0.57
2QZ J222006.7−280324	2.414	47.22	13	16	44.63	44.73	1019	908	45.14	0.42
[HB 89] 2254+024	2.083	46.45	15	13	43.94	43.86	612	1390	44.78	1.27
2QZ J231456.8−280102	2.400	46.31	15	15	43.79	43.81	1267	1654	44.47	<0.1
2QZ J234510.3−293155	2.382	46.32	20	28	43.96	44.11	887	758	44.79	0.82

NOTE.—The methods used to obtain best fit and direct measurements are outlined in Paper I.
[a] Systemic redshift (see Paper I).

Very high luminosity sources that are also weak [O III] λ5007 emitters have been found by Yuan & Wills (2003) in their IR study of high-redshift quasars. However, most of those objects are broad absorption line quasars (BALQSOs) that are known to have a weak [O III] λ5007 line. Regarding intermediate-luminosity AGNs, BG92 find that 26 of the 87 sources in their PG quasar sample show EW ([O III] λ5007) < 10 Å, and 12 show EW ([O III] λ5007) < 6 Å. In addition, about half of the quasars in the new Sulentic et al. (2004) high-z sample have EW ([O III] λ5007) < 6 Å. Assuming the upper limits we obtained can be translated to actual EW measurements, we conclude that the EW distribution in our sample is not very different from that of BG92. Combining this with the information about nearby Seyfert 1 galaxies, we conclude that there are very few weak [O III] λ5007 emitters among low-luminosity AGNs, but their fraction increases toward intermediate and high luminosity. However, $L_{[O\ III]}$ of the very luminous sources in our sample is 2 orders of magnitude larger than observed in the most luminous BG92 objects. This has important implications for the physics and the structure of the NLR in these extreme cases, as discussed in §§ 3–4.

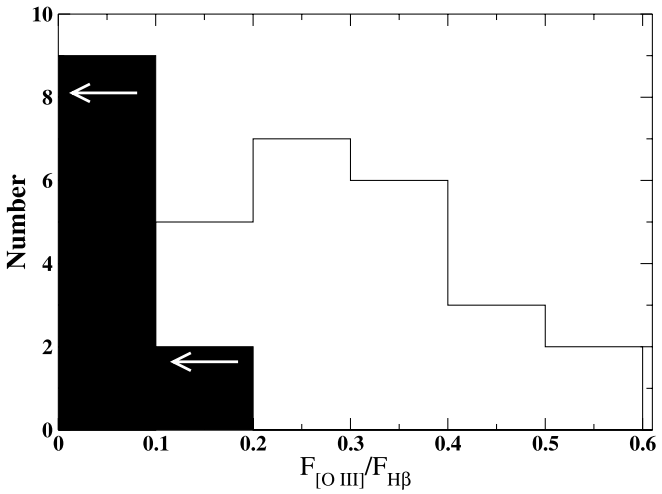

FIG. 2.—[O III] λ5007/Hβ line ratio histogram for our sources. The dark region indicates sources with upper limits (*arrows*) on the [O III] λ5007 flux.

3. LUMINOSITY, EQUIVALENT WIDTH, AND SIZE CORRELATIONS

3.1. *Measured and Predicted NLR Sizes*

B02 measured NLR sizes in seven PG quasars and compared them with sizes obtained by Falcke et al. (1998) in nearby Seyfert 2 galaxies. Their main finding is a strong correlation between the NLR radius (R_{NLR}) and the [O III] λ5007 line luminosity. Their relationship (B02 eq. [1]), scaled

to the somewhat different cosmology adopted here, can be written as

$$R_{\rm NLR} = 2.1 L_{[\rm O\ III],42}^{0.52\pm0.06}\ \rm kpc, \quad (1)$$

where $L_{[\rm O\ III],42} = L_{[\rm O\ III]}/10^{42}$ ergs s^{-1}. This is in perfect agreement with $R_{\rm NLR} \propto L_{[\rm O\ III]}^{1/2}$ (the uncertainty on the constant 2.1 kpc is of order 15%). For reasons that will become apparent later, we prefer to use the equivalent relation involving the Hβ luminosity (B02 eq. [3] converted to our assumed cosmology),

$$R_{\rm NLR} = 1.15 L_{\rm H\beta,42}^{0.49\pm0.06}\ \rm kpc, \quad (2)$$

where $L_{\rm H\beta,42} = L_{\rm H\beta}/10^{42}$ ergs s^{-1}.

The recent, more detailed work of Schmitt et al. (2003) uses a sample of 60 Seyfert 1 and Seyfert 2 galaxies and discuss in detail the differences between the two subgroups, the concentration of the [O III] λ5007 emission, and other properties. The main finding that is relevant to our work is the following relationship (adjusted to the cosmology used here):

$$R_{\rm maj} \simeq 1.2 L_{[\rm O\ III],42}^{0.33\pm0.04}\ \rm kpc, \quad (3)$$

where $R_{\rm maj}$ is the size of the semimajor axis of the [O III] λ5007 nebulosity. This is significantly different from the B02 results in both the *R-L* dependence and the normalization. Schmitt et al. (2003) have also investigated the correlation when the seven B02 sources are added to their sample. The result is a steeper dependence of the form $R_{\rm maj} \propto L_{[\rm O\ III]}^{0.42}$. A new work by Bennert et al. (2004) argues that much of the difference is due to orientation, since most of the sources in Schmitt et al. (2003) are Seyfert 2 galaxies while the more luminous sources in B02 are all type 1 AGNs. We return to this issue in § 4.

Theoretical suggestions that the NLR size should scale with $L_{\rm ion}^{1/2}$, where $L_{\rm ion}$ is the ionizing source luminosity, have been discussed in many papers (see Netzer 1990 for references prior to 1990 and Dopita et al. 2002 for more recent publications). This is based on the assumption that both the broad-line region (BLR) gas and the NLR gas are photoionized by a central source whose spectral energy distribution changes only slightly with source luminosity. Spectroscopic studies show a remarkable similarity between the emission-line spectrum of high- and low-luminosity AGNs. This suggests that the ionization parameter U (defined here as the ratio of the Lyman continuum photon density to the hydrogen number density $N_{\rm H}$) and the typical gas density are basically the same in all sources. Since $U \propto L_{\rm ion}/N_{\rm H}R^2$, we find $R \propto L_{\rm ion}^{1/2}$. An additional assumption is that most of the [O III] λ5007 emission originates in radiation-bounded clouds because of the fairly uniform value of I ([O III] λ5007)/I (narrow Hβ). This allows us to replace $L_{\rm ion}$ by the luminosity of any hydrogen recombination line, e.g., Hβ. We note that there is a well-established *R-L* correlation for the BLR gas (e.g., Kaspi et al. 2000), where reverberation mappings show that $R_{\rm BLR} \propto L^{0.6\pm0.1}$.

A real physical explanation of any *R-L* dependence is still lacking, since the mechanism controlling the gas density and location is unknown. Some papers assume a stratified, radiation bounded NLR with a prechosen run of density and hence level of ionization (e.g., Netzer 1990; Komossa & Schulz 1997). Such models are naturally normalized in incident flux units ($L_{\rm ion}/R^2$) and can be tuned to produce the same mean U for all sources. However, some narrow emission lines are probably produced in density bounded gas (e.g., Binette et al. 1996), which considerably complicates the models. It is also clear (e.g., Alexander et al. 1999) that well-studied NLRs contain a large range of conditions with a spread in ionization parameter and gas density. An almost orthogonal approach is provided by the "locally optimally emitting cloud" (LOC) model (Ferguson et al. 1997). The assumption in this case is of a large range of conditions (density and covering factor) at each location, where the intensities of the various lines reflect the line production efficiency at each location. This efficiency is the highest for densities that are close to the critical density of the line in question. The model provides a natural scaling of $L_{\rm ion}$ with $R_{\rm NLR}$, provided there is a large reservoir of gas with similar properties in all AGNs and on all scales. Finally, there are equally complex NLR models in which shock-excited gas contributes significantly to the observed NLR emission (e.g., Contini et al. 1998; Schiano 1986; Dopita & Sutherland 1995) but no natural *R-L* scaling.

The recent papers by Dopita et al. (2002) and Groves et al. (2004) provide a more solid foundation for NLR modeling. These authors assumed dusty, stratified NLR clouds where the external radiation pressure acts mostly on the dust particles and forces the local ionization parameter to certain specific values such that in the [O III] λ5007–producing gas, $U \simeq 10^{-2}$. The model suggests a natural $R_{\rm NLR} \propto L^{1/2}$ dependence. It also implies that the composition and temperature of the gas are rather different from those assumed in other models because of metal depletion.

3.2. *New* [O III] *and* $R_{\rm NLR}$ *Measurements*

The combination of B02 observations and recent theoretical developments points to a "natural" $R_{\rm NLR} \propto L_{\rm ion}^{1/2}$ dependence yet raises a severe problem regarding the NLR size in high-luminosity AGNs. Any such scaling will lead, at large enough $L_{\rm ion}$, to sizes that are larger than galactic sizes. The B02 results addressed here are used for normalizing this relationship, but the problem exists at high luminosity regardless of whether their scaling is correct. Given this, we would not expect to see any strong [O III] λ5007 emitters in high-luminosity sources, yet our new observations clearly show such objects.

To define the problem in a more quantitative way we plot in Figure 3 three quantities versus $L_{\rm H\beta}$ (luminosity of the entire emission line). The first is the measured $R_{\rm NLR}$ from the B02 sample (seven sources) where we also show the best (modified) B02 fit (eq. [2]). The second is from our newly observed Hβ and [O III] λ5007 lines with two additional sources from Dietrich et al. (2002a). For these we use equation (1) *to guess* $R_{\rm NLR}$, given the observed $L_{[\rm O\ III]}$. The predicted $R_{\rm NLR}$ for most sources in this group lies close to the value predicted from $L_{\rm H\beta}$ (*straight line*), confirming the small scatter in I ([O III] λ5007)/I (Hβ). The third group includes the seven sources from our sample and the four sources from Dietrich et al. (2002a), where no [O III] λ5007 has been detected. For these we use $R_{\rm NLR}$ derived from the upper limits on $L_{[\rm O\ III]}$. The upper limits on $R_{\rm NLR}$ obtained in this way are a factor of 2–3 smaller than those derived from $L_{\rm H\beta}$.

The implications of Figure 3 are clear. For those sources with measured Hβ and [O III] λ5007 lines, the derived $R_{\rm NLR}$ is enormous, exceeding 70 kpc in the most luminous sources. We consider those sizes completely unreasonable for reasons that are discussed in § 4. As in Figure 2, this diagram suggests a dichotomy in the properties of the high-luminosity quasars, where some sources show strong [O III] λ5007 lines and others show no or very weak such emission.

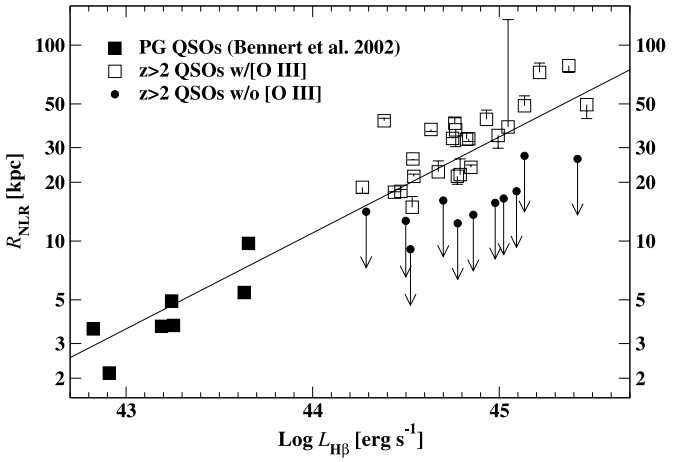

FIG. 3.—The R_{NLR} vs. $L_{H\beta}$ diagram including our luminous high-z quasars. Filled squares are the original B02 quasar data, and the straight line is the B02 R_{NLR}-$L_{H\beta}$ best-fit line. Open symbols represent high-z quasars with measured [O III] lines, for which R_{NLR} was *inferred* from the B02 R_{NLR}-$L_{[O\ III]}$ relation. One-sided error bars on the open symbols indicate the difference between best-fit and "direct" measurements (see text). Arrows represent high-z quasars, for which we have an upper limit on the [O III] λ5007 line flux and hence a limit on R_{NLR} from the B02 relation. Note the two distinct groups and the enormous predicted R_{NLR} at high-Hβ luminosity.

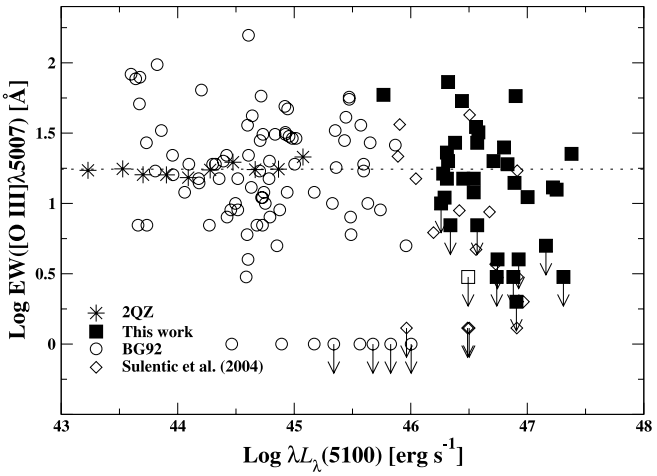

FIG. 5.—Baldwin relationship for [O III] λ5007. Mean (over luminosity bins) values for the Croom et al. (2002) 2QZ sources are marked with asterisks. The data presented in this paper are marked with filled squares. The BG92 and Sulentic et al. (2004) samples are marked with circles and diamonds, respectively. Upper limits on EW ([O III] λ5007) are marked with arrows. The mean EW ([O III] λ5007) of the 2QZ sample is marked by a dotted line.

There are two other ways to verify, experimentally, the B02 claim. Most of our sample is at $z \simeq 2.5$. At this redshift, and the chosen cosmology, the angular diameter distance is a weak function of redshift and corresponds to about 7 kpc arcsec^{-1}. The predicted R_{NLR}, using the B02 relationships and our measured [O III] λ5007 luminosities, corresponds to a total extent of 2″–10″. This can be tested by spatially resolved space and ground-based observations. The two-dimensional spectra of two of our sources ([HB 89] 0329−385 and 2QZ J222006.7−280324) show prominent [O III] λ5007 emission, which allows such measurements (see Fig. 4). In these cases, most of the line flux (>99%) is emitted within the central 4 pixels corresponding to a radius of 7.2 kpc at each source. This size is a strong upper limit, since much of the flux is likely to be due to the point-spread function (corresponding to ∼1″ at the time of observations). The two upper limits on R_{NLR} obtained in this way are a factor of ∼5 smaller than the radii derived from the B02 relationships.

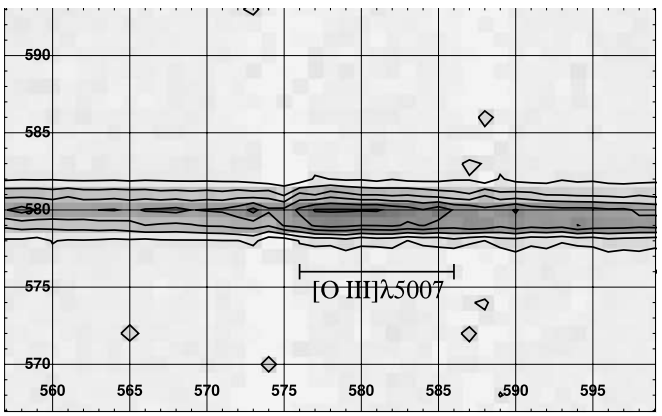

FIG. 4.—Two-dimensional spectrum around the [O III] λ5007 region of 2QZ J222006.7−280324. The coordinates of the vertical and horizontal axes are given in pixels, where each pixel in the spatial (vertical axis) corresponds to 0.″446 (∼3.5 kpc). Note that there is no trace of extended [O III] λ5007 emission beyond a ∼1″ (∼7.2 kpc) radius from the center.

The term "NLR radius" used by B02 is ambiguous since those authors used very low surface brightness features to define the dimension of the [O III] λ5007 nebulosity. We used the *HST* archive to extract and reanalyze the B02 images. In particular, we examined the source showing the largest [O III] λ5007 nebulosity, PG 1049−005, and remeasured its observed [O III] λ5007 image. We found that 95% of the line emission is encircled within a radius of 1.″1, which corresponds to a radius of 5.5 kpc at the source. This is half of the radius deduced by B02 and suggests that the bulk of the NLR emission is emitted within a volume that is much smaller than inferred by their relationships. The different way of measuring the [O III] λ5007 nebulosity is probably the main source of discrepancy in normalization (i.e., the NLR radius at $L_{[O\ III],42} = 1$) between the B02 and the Schmitt et al. (2003) works.

In summary, our new observations contradict the B02 results in two ways. First, about one-third of the high-luminosity sources show no trace of an NLR. Second, there are direct indications in three cases and sound theoretical reasons (see below) for suggesting that most of the NLR emission is restricted to a volume that is much smaller than inferred from the B02 relationships.

3.3. *The Baldwin Relationship for* [O III]

The new data show the presence of two groups of luminous AGNs, those with strong [O III] λ5007 and those with no (or very weak) such line. Of the 35 sources investigated by us (six from Dietrich et al. 2002a and 29 from our IR sample), 24 belong to the first group and 11 to the second. As mentioned above, earlier studies such as Yuan & Wills (2003) already found very weak [O III] λ5007 in several AGNs. Most or all of these are known BALQSOs, while only two of the 10 sources discussed here (one, [HB 89] 0105−265, from Dietrich et al. 2002a, and one, [HB 89] 1246−057, from our sample) show BALQSO properties. Thus, weak or no [O III] λ5007 seems to be a common property of many luminous AGNs.

To further illustrate this point we plot in Figure 5 EW ([O III] λ5007) versus λL_λ (5100 Å) for the high-z quasars from our sample and that of Sulentic et al. (2004), for which B magnitudes were transformed to λL_λ (5100) assuming $L_\nu \propto \nu^{-\alpha}$ with

TABLE 2
SPEARMAN RANK CORRELATION COEFFICIENTS MATRIX

Property versus	M_{BH}	L/L_{Edd}	Fe II/Hβ	EW ([O III])	EW (Hβ)
$\lambda L_\lambda(5100)$	0.85*[a]	0.48*[a]	−0.04[b]	−0.09[c]	−0.37*[d]
M_{BH}	...	0.03[a]	−0.22[e]	0.14[f]	−0.15[a]
L/L_{Edd}	...	...	0.48*[e]	−0.13[f]	−0.47*[a]
Fe II/Hβ	...	...	...	−0.39*[g]	−0.33*[b]
EW ([O III])	...	...	...	...	0.28*[c]
EW (Hβ)	...	...	...	...	...

NOTES.—Significant correlations with chance probabilities smaller than 1% are marked with asterisks. Upper limits were not included in the correlations.
[a] 118 sources from BG92 and this work.
[b] 124 sources from BG92, Sulentic et al. 2004, and this work.
[c] 121 sources from BG92, Sulentic et al. 2004, and this work.
[d] 135 sources from BG92, Sulentic et al. 2004, and this work.
[e] 107 sources from BG92 and this work.
[f] 104 sources from BG92 and this work.
[g] 110 sources from BG92, Sulentic et al. 2004, and this work.

$\alpha = 0.5$. We also included the BG92 sample in the diagram, and the 2QZ data of Croom et al. (2002), for which b_J magnitudes were transformed to $\lambda L_\lambda(5100)$ using the same methods as above. The diagram shows that for the population of strong [O III] λ5007 emitters, there is no reduction of EW ([O III] λ5007) with source luminosity. On the other hand, there are many weak or no [O III] λ5007 emitters at high luminosity that could give the impression that the line EW decreases with increasing source luminosity. [In fact, the Croom et al. 2002 data represent mean EW ([O III] λ5007) in several luminosity bins. Assuming a fraction of weak [O III] λ5007 emitters in those bins similar to the one found by BG92, we find that the plotted average may underestimate the typical EW ([O III] λ5007) in those sources by about 25%.] We suspect that the Dietrich et al. (2002b) claim of a Baldwin relationship for this line is the result of their averaging together four very weak [O III] λ5007 emitters with two sources showing typical EW ([O III] λ5007).

For completeness, we also tested the correlation of EW ([O III] λ5007) with accretion rate (in terms of the L_{Bol}/L_{Edd} ratio, hereafter L/L_{Edd}; see Paper I for more details). Correlations with accretion rate are found to be extremely important in Paper I and in § 3.5. For EW ([O III] λ5007), this correlation is not significant (see Table 2).

3.4. *FWHM Correlations*

We have tested our sample for possible correlations of luminosity, black hole (BH) mass, and accretion rate with FWHM ([O III] λ5007). Such correlations have been investigated in the past (e.g., Shields et al. 2003), and FWHM ([O III] λ5007) has been suggested as a potentially useful surrogate for σ_*.

Figure 6 shows FWHM ([O III] λ5007) versus source luminosity, M_{BH}, and L/L_{Edd} for our sample and the Shields et al. (2003) sources. To obtain the intrinsic line width, we assumed

$$\Delta\lambda^2_{true} = \Delta\lambda^2_{obs} - \Delta\lambda^2_{inst}, \quad (4)$$

where $\Delta\lambda_{inst}$ is the instrumental resolution. Since the slit width and the seeing disk sizes were comparable during the time of observations, this is a reasonable assumption for line profiles that are indistinguishable from a Gaussian. The uncertainty on FWHM ([O III] λ5007) is quite large for the poorer S/N spectra and is of the order of the instrumental (or rebinned instrumental) resolution ($\sim$600 km s^{-1}). BH masses and L/L_{Edd} for all sources on these diagrams were calculated as prescribed in Paper I.

On their own, the measured FWHM ([O III] λ5007) for our high-z sources show no correlation with luminosity, BH mass, or accretion rate because of the narrow luminosity range of our sample. The additional Shields et al. (2003) data increase this range considerably and show significant correlations with all three parameters. The strongest correlation is between FWHM ([O III] λ5007) and luminosity. The strength of the correlation increases with the dependence on luminosity, i.e., less significant correlations as one goes from L to M_{BH} ($\propto L^{0.6}$) to L/L_{Edd} ($\propto L^{0.4}$).

3.5. *Correlations Involving* Hβ *and* Fe II

In Paper I and in Table 1 we give $L_{H\beta}$, which we transformed to EW (Hβ), and Fe II/Hβ. Here again we have tested the correlations of these quantities against L, M_{BH}, and L/L_{Edd}

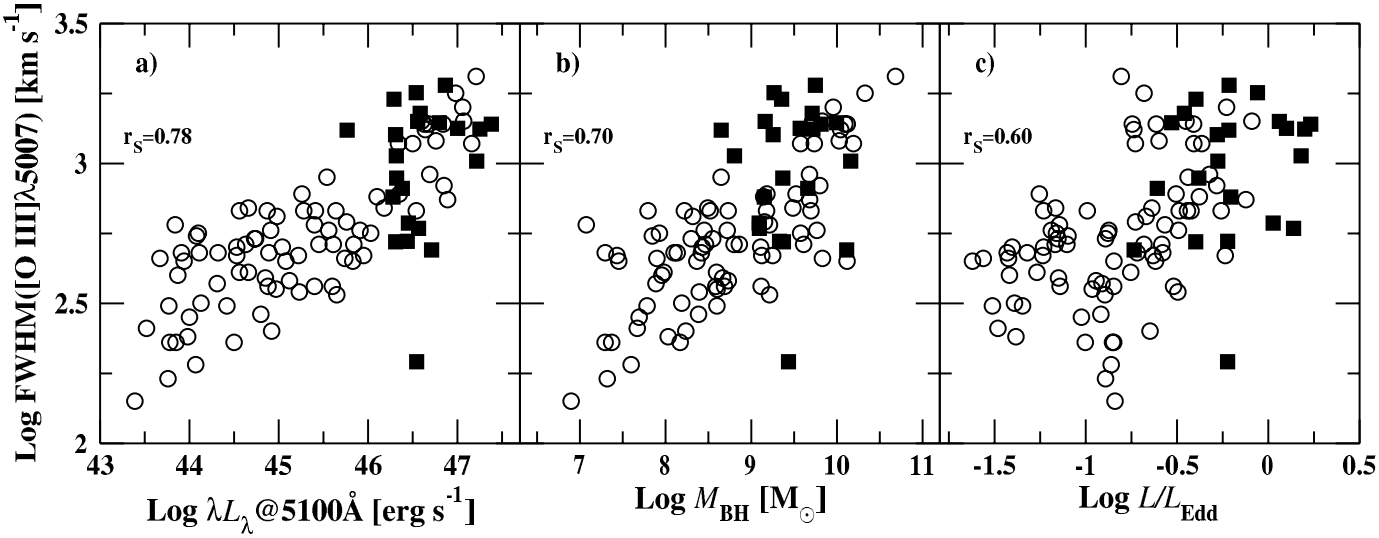

FIG. 6.—FWHM ([O III] λ5007) vs. (*a*) $\lambda L_\lambda(5100)$, (*b*) M_{BH}, and (*c*) L/L_{Edd} for the Shields et al. (2003) sample (*open symbols*) and the high-z quasars presented in this paper (*filled symbols*). The strongest correlation is between FWHM ([O III] λ5007) and luminosity. The correlation weakens as the dependence on luminosity drops from L through M_{BH} ($\propto L^{0.6}$) to L/L_{Edd} ($\propto L^{0.4}$), as indicated by the Spearman rank correlation coefficients at the top left of each panel.

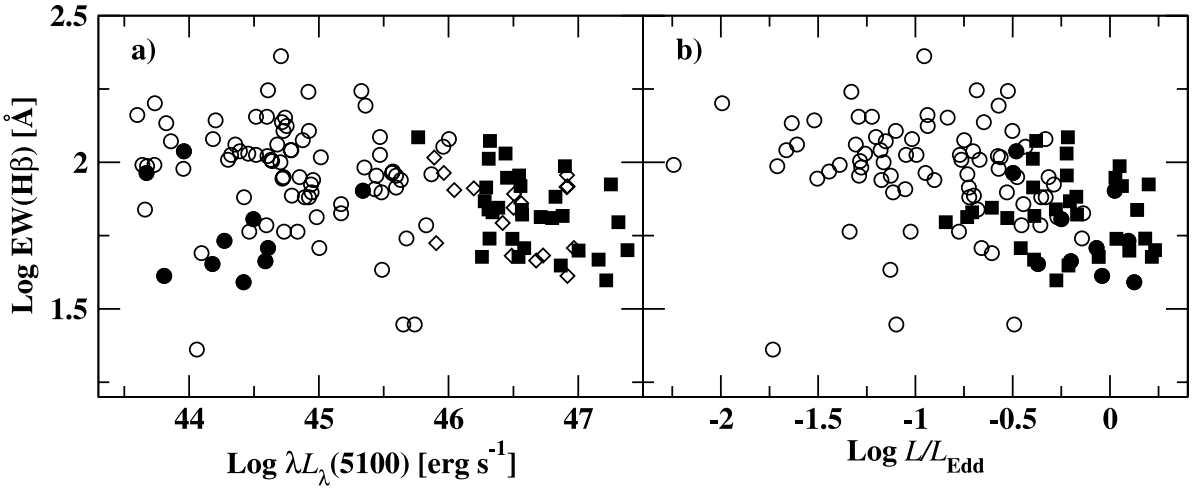

FIG. 7.—EW (Hβ) vs. (*a*) luminosity and (*b*) $L/L_{\rm Edd}$ for the BG92 sample (including broad-line AGNs [*open circles*] and NLS1s [*filled circles*]), the Sulentic et al. (2004) sample (*open diamonds* in [*a*]) and the high-*z* quasars presented in this paper (*filled squares*).

using our sample and the samples of Sulentic et al. (2004) and BG92 (accretion rates for the BG92 sample were calculated as prescribed in Paper I). For EW (Hβ) we find significant correlations with both L and $L/L_{\rm Edd}$. Details of the correlations are given in Table 2 and in Figure 7. In the case of Fe II/Hβ the only significant correlation is with $L/L_{\rm Edd}$. Details of those correlations are also given in Table 2. Figure 8 shows the strongest correlation of Fe II/Hβ (against the accretion rate) for our new sources combined with those of BG92.

The Baldwin relationship found here for EW (Hβ) and shown in Figure 7 is interesting, since it is in contradiction with the Croom et al. (2002) finding for this line. However, our combined sample is far from being complete, in particular at the high-luminosity range where we specifically chose to observe high-luminosity sources. Thus, it is likely that lower luminosity sources at high redshift would have a larger EW (Hβ) that will spoil the correlation. Regarding the dependence on accretion rate, similar selection effects may be operating, but the observed correlation is so strong that we suggest that this may be a real effect. We also note that in Figure 7 the narrow-line Seyfert 1 galaxies (NLS1s) are situated very close to the high-luminosity, high accretion rate sources. The situation resembles the Baskin & Laor (2004) finding that EW (C IV λ1549) depends strongly on $L/L_{\rm Edd}$ even in low-luminosity AGNs that do not show the Baldwin relationship for this line.

Figure 8 is hard to interpret. Considering only sources with measurable Fe II/Hβ (i.e., a ratio larger than $\sim$0.1) we find a clear trend of increased Fe II/Hβ for higher accretion rates (see Table 2). In particular, we note the similar location on the diagram of our high-*z* quasars and the NLS1s. However, there is a significant number of sources with very small Fe II/Hβ and very large $L/L_{\rm Edd}$. We note in this respect that our new observations extend the measurement of Fe II/Hβ to values of $L/L_{\rm Edd}$ never investigated before. The only exceptions, perhaps, are a few BALQSOs in the Yuan & Wills (2003) sample with spectral properties very different from those of our (non-BAL)

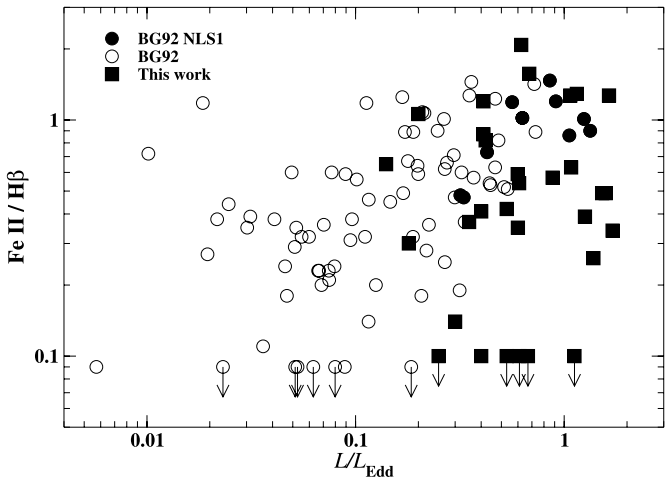

FIG. 8.—Fe II/Hβ vs. $L/L_{\rm Edd}$ for the BG92 sample and the high-*z* quasars presented in this paper (symbols are similar to those in Fig. 7). Arrows represent no detection of iron emission (in the BG92 sample the upper limit on the Fe II/Hβ ratio was set to 0.09, which is the lowest value they reported, and in our sample the upper limits are given in Table 1).

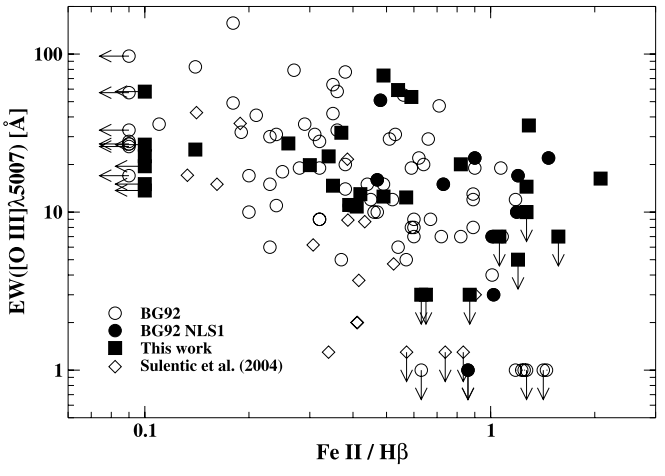

FIG. 9.—EW ([O III] λ5007) vs. Fe II/Hβ for the BG92 sample, the Sulentic et al. (2004) sample, and the high-*z* quasars presented in this paper (symbols are similar to those in Fig. 7). Upper limits on Fe II/Hβ (*arrows pointing left*) are similar to those shown in Fig. 8. Upper limits on EW ([O III] λ5007), i.e., no [O III] λ5007 detection, for the BG92 (Sulentic et al. 2004) sample were set to 1 (1.3) Å, which is the lowest value each of them reported. The upper limits on EW ([O III] λ5007) for our sample are given in Table 1.

sources (note that these authors measured the entire optical Fe II blends, and their values must be scaled down by a factor of 3.58 for comparison with the measurements presented in our work; B. Wills 2004, private communication).

The above two findings suggest that the main reason for the increase of Fe II/Hβ with the accretion rate is the decrease of EW (Hβ) with $L/L_{\rm Edd}$. In fact, looking at EW (Fe II) against $L/L_{\rm Edd}$ (not shown here) we find no correlation at all. The fractional increase in Fe II/Hβ with accretion rate is also consistent with the decrease in EW (Hβ). However, we cannot rule out the possibility that changes in the Fe/H abundance ratio are involved too, as is shown in Paper I to be the case for N/C.

In Figure 9 we plot the well-known anticorrelation between EW ([O III] λ5007) and Fe II/Hβ (e.g., BG92) for our sources, for the low-z BG92 sources, and for the new intermediate-z sample of Sulentic et al. (2004). Our sources are consistent with this trend. Fe II/Hβ for our sources is generally higher than in BG92 and Sulentic et al. (2004), indicating, perhaps, the strong dependence of this property on the total luminosity. However, there are clear exceptions, i.e., sources with very high luminosity, yet relatively small Fe II/Hβ. Here again we note similar large values of Fe II/Hβ in several of the BALQSOs of Yuan & Wills (2003).

4. DISCUSSION

4.1. *Do Enormous NLRs Really Exist?*

A major goal of the present investigation is to test the NLR properties and the NLR spectrum in very high luminosity sources where the theoretically predicted $R_{\rm NLR}$, as well as the empirical B02 relationship, results in unreasonably large dimensions. The B02 sample already included claims for sources with $R_{\rm NLR} \sim 10$ kpc, and our bright [O III] λ5007 emitters would continue this relationship to enormously large NLRs (more than 100 kpc in diameter; see Fig. 3). There are, however, fundamental problems in this suggested size-luminosity interpretation on both observational and theoretical grounds.

B02 suggested two estimates of the NLR size (eqs. [1] and [2]). We separate the discussion of those claims into two, according to the two subgroups discovered here (the weak and the strong [O III] λ5007 emitters). For the weak [O III] λ5007 emitters we find a clear contradiction between the $R_{\rm NLR}$ based on the observed Hβ luminosity and the one based on the observed (or the upper limit on) [O III] λ5007 luminosity (Fig. 3). As for the strong [O III] λ5007 emitters, two-dimensional spectra of two of our sources rule out the large predicted dimensions (§ 3.2). Moreover, our new measurements of the largest [O III] λ5007 nebula in the B02 sample are also in conflict with the B02 relationships. Based on the evidence at hand, we suspect that the $R_{\rm NLR} \propto L_{\rm ion}^{1/2}$ dependence breaks down at some intermediate luminosity scale and that the "true" NLR radius, defined here as the radius encompassing 95% of the line emission, does not exceed a few kiloparsecs even in the most luminous quasars.

There are other predictions that make us question the existence of such enormous NLRs. The suggested $R_{\rm NLR} \propto L_{\rm ion}^{1/2}$ relationship would predict NLR sizes, in the most luminous AGNs, that exceed the size of the largest known bulges and, in fact, the size of the largest known galaxies (except for some cD galaxies). Such sizes are unacceptable for several reasons. First, the escape velocity from a spherical galaxy is roughly $290 M_{11}^{1/2} R_{10\,\rm kpc}^{-1/2}$ km s^{-1}, where M_{11} is the mass in units of $10^{11}\ M_\odot$ and R_{10} is the radial distance in units of 10 kpc. The new FWHMs listed in Table 1 and shown in Figure 6, compared with the predicted $R_{\rm NLR}$, suggest therefore dynamically unbounded NLRs. Given those velocities and dimensions, the dynamical time for the most luminous [O III] λ5007 emitters is a few $\times\ 10^7 R_{10}$ yr, suggesting a short-lived phenomenon. The inferred amount of ionized gas in such NLRs, given radiation bounded gas and a typical ionization parameter, is

$$M_{\rm NLR} \simeq 10^9 \left(\frac{C_f}{0.1}\right) R_{10}^2 N_{21}\ M_\odot, \qquad (5)$$

where C_f is the covering fraction and N_{21} is the column density in units of 10^{21} cm^{-2}. Simple photoionization arguments show that for strong [O III] λ5007 emitters $N_{21} > 1$. This would give $M_{\rm NLR} > 10^9\ M_\odot$ for all of our sources and $M_{\rm NLR} > 10^{10}\ M_\odot$ for the most luminous [O III] λ5007 emitters. Judging by the observed FWHM, most of this material is probably unbound and thus flows from the center at outflow rates approaching $10^6 R_{10}^2\ M_\odot$ yr^{-1} assuming a density of $\sim 10^3$ cm^{-3}. All those numbers seem incompatible with long-term mass ejection in AGN-hosting galaxies.

The Schmitt et al. (2003) results alleviate some of these difficulties because of the smaller size normalization and the flatter $R_{\rm NLR}$-$L_{\rm [O\,III]}$ dependence. However, it is not at all clear that extrapolating their results to much higher luminosity with the suggested $L^{1/3}$ dependence (eq. [3]) is justified in view of the B02 measurements.

We are facing a situation in which sound physical arguments (e.g., the narrow-line spectrum and the Groves et al. 2004 dusty NLR model) support the expected $R_{\rm NLR} \propto L^{1/2}$ relationship, yet its application to the most luminous quasars gives unreasonably large sizes, masses, and mass outflow rates. As explained below, the most likely explanation in our opinion is that typical NLRs (i.e., those similar in their properties to the ones observed in Seyfert 1 galaxies) cannot last very long in high- and perhaps also in intermediate-luminosity AGNs. This means that the [O III] λ5007–emitting regions in our sample may be of a different origin and physical properties.

4.2. *Luminous NLRs as Star-forming Regions*

If compact NLRs are indeed typical of many high-luminosity AGNs, then their properties must be very different from the properties of those NLRs observed in nearby sources. In particular, the gas density in the highest luminosity NLRs must be several orders of magnitude larger. Consider, for example, a maximum NLR size of $\sim$3 kpc and assume a similar ionization parameter in all NLRs. This would mean that the gas density in the most luminous [O III] λ5007 emitters is 10^2–10^3 times larger than the density in nearby Seyfert 1 galaxies. The spectroscopic properties must be very different too, which can, in principle, be tested by accurate observations. Unfortunately, present-day IR spectroscopy is very limited in this respect because of the restricted wavelength bands available to ground-based observations.

A possible origin of a high-density gas in kpc scale nuclear regions is violent star-forming activity. Such events can produce high-density, large column density, nonsolar composition dusty gas. The overall spectrum of such regions is likely to differ from the spectrum of nearby, lower density NLRs. At present we can only observe [O III] λ5007, which is the strongest emission line under a variety of conditions. Future space-born spectroscopy will be able to test this idea by looking for other emission lines.

The scenario we propose to explain the observations of our high-luminosity AGNs, and the apparent breakdown of the $R_{\rm NLR} \propto L_{\rm ion}^{1/2}$ relationship, is of two distinct populations. For the first, such scaling continues to high luminosity due to radiation pressure force or other effects. This results in short-lived enormous NLRs that will show basically no nuclear narrow emission lines during most of their life. The other group is those sources where a starburst or another unknown process ejects high-density gas into their nuclear region. This gas is ionized and excited by the central radiation source and produces the observed strong [O III] λ5007 lines. Such "star-forming NLRs" would have spectral properties that are rather different from those observed in nearby, less luminous sources. Given the similar fraction of weak [O III] λ5007 emitters in BG92 and in our new sample, we suggest that the phenomenon is of a continuous nature and starts at some intermediate luminosity. Its clearest manifestation is in the highest luminosity sources such as the ones observed here.

4.3. *Correlations Involving* Fe II, Hβ, *and* [O III]

The sample used here, which combines data from various different sources, is not complete. However, it allows the best test so far of the BG92 Fe II/Hβ–[O III] λ5007 relationship and several other suggested correlations at the high end of the AGN luminosity function. The results presented here suggest that the most extreme values of Fe II/Hβ require very high luminosity. They also suggest that a higher accretion rate results in larger Fe II/Hβ (Fig. 8) and that $L/L_{\rm Edd}$ is the most important factor for determining several other correlations. There are, however, some exceptions, i.e., sources with large $L/L_{\rm Edd}$ yet small Fe II/Hβ. Our work shows that the decrease of EW (Hβ) with increasing $L/L_{\rm Edd}$ in the present sample is probably the cause of the increase of Fe II/Hβ with the accretion rate. EW (Fe II) by itself does not depend on the accretion rate, and it is therefore possible that the iron-to-hydrogen abundance ratio plays no role in this correlation. On the other hand, we do not have the data or a good enough theory (e.g., Verner et al. 2004 and references therein) to completely rule out the possibility that the iron abundance depends on luminosity or on the accretion rate. In a similar way, EW ([O III] λ5007) is *not* correlated with $L/L_{\rm Edd}$, but we suggest that the Fe II/Hβ–EW ([O III] λ5007) anticorrelation is driven by the accretion rate.

Sulentic et al. (2004) and others argued that the general AGN population should be divided into two subgroups according to the so-called eigenvector 1 (E1; see BG92), which contains four main observables. According to this scheme, group A sources show the strongest E1 properties. Most radio-loud AGNs belong to group B, i.e., those with weaker E1 properties. Here we are not interested in E1 as such since our sample is not complete and so is the combination of our sample with the BG92 and the Sulentic et al. (2004) samples. We are, however, in a position to look at the extreme end of the distribution in L and in $L/L_{\rm Edd}$ and test for those quantities that depend on them. We have already discussed all the relevant correlations. Here we note that all those involving $L/L_{\rm Edd}$ show that NLS1s occupy the same part of parameter space as the high-luminosity, high accretion rate AGNs observed by us. These sources are thus the high-luminosity analogs of NLS1s and should perhaps be referred to as narrow-line type 1 quasars (NLQ1s).

5. CONCLUSIONS

We have discussed the near-IR spectra of 29 newly observed high-luminosity, high-redshift AGNs and used the data to argue that previous claims for expected and observed $R_{\rm NLR} \propto L_{\rm [O\,III]}^{1/2}$ dependence are in conflict with the observations. About two-thirds of all very high luminosity sources show strong [O III] λ5007 lines, while the remaining objects show no or very weak such lines. We suggest that the NLR properties in high-luminosity, strong [O III] λ5007 emitters are very different from those observed in nearby AGNs and possibly imply denser than "usual" NLRs. The origin of the high-density gas is likely to be a violent star-forming event in the nucleus. We also investigated Fe II/Hβ and EW ([O III] λ5007) at the high end of the luminosity and $L/L_{\rm Edd}$ in AGNs and showed that the first of those is probably driven by the overall accretion rate while the second is independent of source luminosity (i.e., no Baldwin relationship) or accretion rate. The Fe II/Hβ ratio may be an iron abundance indicator, but this cannot be proven observationally because of the EW (Hβ) dependence on accretion rate.

We are grateful to the technical staff at the Anglo-Australian Telescope (AAT) and Italian Telescopio Nazionale Galileo (TNG) observatories for invaluable help during the observations. This work is based on observations made with the TNG operated on the island of La Palma by the Centro Galileo Galilei of the Istituto Nazionale di Astrofisica (INAF) at the Spanish Observatorio del Roque de los Muchachos of the Instituto de Astrofisica de Canarias. We would like to thank Angela Cotera for allowing us to use half a night of her time at AAT, and Dirk Grupe for providing us an electronic version of the Boroson & Green (1992) Fe II template. We gratefully acknowledge constructive remarks from an anonymous referee, who helped to improve this work considerably. The Two-Degree Field QSO Redshift Survey (2QZ) was compiled by the 2QZ survey team from observations made with the Two-Degree Field on the AAT. Funding for the creation and distribution of the SDSS Archive has been provided by the Alfred P. Sloan Foundation, the Participating Institutions, the National Aeronautics and Space Administration, the National Science Foundation, the US Department of Energy, the Japanese Monbukagakusho, and the Max Planck Society. The SDSS Web site is http://www.sdss.org. The SDSS is managed by the Astrophysical Research Consortium (ARC) for the Participating Institutions. The Participating Institutions are the University of Chicago, Fermilab, the Institute for Advanced Study, the Japan Participation Group, the Johns Hopkins University, Los Alamos National Laboratory, the Max-Planck-Institute for Astronomy (MPIA), the Max-Planck-Institute for Astrophysics (MPA), New Mexico State University, University of Pittsburgh, Princeton University, the United States Naval Observatory, and the University of Washington. This research has made use of the NED database, which is operated by the Jet Propulsion Laboratory, California Institute of Technology, under contract with the National Aeronautics and Space Administration. This work is supported by Israel Science Foundation grant 232/03. R. M. acknowledges partial support by the Italian Ministry of Research (MIUR).

REFERENCES

Alexander, T., Sturm, E., Lutz, D., Sternberg, A., Netzer, H., & Genzel, R. 1999, ApJ, 512, 204
Baldwin, J. A. 1977, ApJ, 214, 679
Barth, A. J., Ho, L. C., Filippenko, A. V., Rix, H., & Sargent, W. L. W. 2001, ApJ, 546, 205
Baskin, A., & Laor, A. 2004, MNRAS, 350, L31

Bennert, N., Falcke, H., Schulz, H., Wilson, A. S., & Wills, B. J. 2002, ApJ, 574, L105 (B02)
Bennert, N., Falcke, H., Shchekinov, Y., & Wilson, A. S. 2004, in IAU Symp. 222, The Interplay among Black Holes, Stars, and ISM in Galactic Nuclei, ed. T. Storchi-Bergmann, L. C. Ho, & H. R. Schmitt (Dordrecht: Kluwer), in press
Binette, L., Wilson, A. S., & Storchi-Bergmann, T. 1996, A&A, 312, 365
Boroson, T. A., & Green, R. F. 1992, ApJS, 80, 109 (BG92)
Contini, M., Prieto, M. A., & Viegas, S. M. 1998, ApJ, 492, 511
Croom, S. M., et al. 2002, MNRAS, 337, 275
Dietrich, M., Appenzeller, I., Vestergaard, M., & Wagner, S. J. 2002a, ApJ, 564, 581
Dietrich, M., Hamann, F., Shields, J. C., Constantin, A., Vestergaard, M., Chaffee, F., Foltz, C. B., & Junkkarinen, V. T. 2002b, ApJ, 581, 912
Dopita, M. A., Groves, B. A., Sutherland, R. S., Binette, L., & Cecil, G. 2002, ApJ, 572, 753
Dopita, M. A., & Sutherland, R. S. 1995, ApJ, 455, 468
Falcke, H., Wilson, A. S., & Simpson, C. 1998, ApJ, 502, 199
Ferguson, J. W., Korista, K. T., Baldwin, J. A., & Ferland, G. J. 1997, ApJ, 487, 122
Groves, B. A., Dopita, M. A., & Sutherland, R. S. 2004, ApJS, 153, 9
Kaspi, S., Smith, P. S., Netzer, H., Maoz, D., Jannuzi, B. T., & Giveon, U. 2000, ApJ, 533, 631
Komossa, S., & Schulz, H. 1997, A&A, 323, 31
McIntosh, D. H., Rieke, M. J., Rix, H.-W., Foltz, C. B., & Weymann, R. J. 1999, ApJ, 514, 40
Nelson, C. H. 2000, ApJ, 544, L91
Nelson, C. H., & Whittle, M. 1996, ApJ, 465, 96
Netzer, H. 1990, in Active Galactic Nuclei, ed. T. J.-L. Courvoisier & M. Mayor (Berlin: Springer), 57
Schiano, A. V. R. 1986, ApJ, 302, 81
Schmitt, H. R., Donley, J. L., Antonucci, R. R. J., Hutchings, J. B., Kinney, A. L., & Pringle, J. E. 2003, ApJ, 597, 768
Shemmer, O., Netzer, H., Maiolino, R., Croom, S., Oliva, T., Corbett, E., & Di Fabrizio, L. 2004, ApJ, 614, 547 (Paper I)
Shields, G. A., Gebhardt, K., Salviander, S., Wills, B. J., Xie, B., Brotherton, M. S., Yuan, J., & Dietrich, M. 2003, ApJ, 583, 124
Sulentic, J. W., Stirpe, G. M., Marziani, P., Zamanov, R., Calvani, M., & Braito, V. 2004, A&A, 423, 121
Veilleux, S. 1991, ApJS, 75, 383
Veilleux, S., & Osterbrock, D. E. 1987, ApJS, 63, 295
Verner, E., Bruhweiler, F., Verner, D., Johansson, S., Kallman, T., & Gull, T. 2004, ApJ, 611, 780
Yuan, M. J., & Wills, B. J. 2003, ApJ, 593, L11